International Journal of Advanced Engineering and Management Research

Vol. 10, No. 01; 2025

ISSN: 2456-3676

Investigating Inhibitory Actions of Expired Omeprazole in Sulphuric Acid as Corrosion Resistance of Mild-steel

Okechukwu Dominic Onukwuli[1], Ifeanyi John Obibuenyi[2]*, Linda Nnodi[3], Uchenna Luvia Ezeamaku[4], Joseph Okechukwu Ezeugo[5], Monday Omotioma[6]

[1]Nnamdi Azikiwe University, PMB 5025, Department of Chemical Engineering, Awka, Anambra State, Nigeria
orcid:0000-0002-0861-3536

[2]Madonna University Nigeria, Department of Chemical Engineering, Faculty of Engineering and Technology, Akpugo Campus, Enugu State, Nigeria
orcid:0000-0001-6283-4711

[3]Odumegwu Ojukwu University, Department of Chemical Engineering, Chukwuemeka, Uli Campus, Anambra State, Nigeria.

[4]Federal University of Technology, PMB 1526, Department of Polymer and Textile Engineering, School of Engineering and Engineering Technology, Owerri, Imo-State, Nigeria
orcid: 0000-0003-1003-9710

[5]Chukwuemeka Odumegwu Ojukwu University, Department of Chemical Engineering, Uli Campus, Anambra State, Nigeria

[6]Enugu State University of Science and Technology, P.M.B. 01660, Department of Chemical Engineering, Enugu, Enugu State, Nigeria
*Corresponding author: * Ifeanyi John Obibuenyi: e-mail address:

doi.org/10.51505/ijaemr.2025.1010 URL: http://dx.doi.org/10.51505/ijaemr.2025.1010

Received: Jan 25, 2025 Accepted: Feb 03, 2025 Online Published: Feb 17, 2025

Abstract

It is proposed to investigate the inhibitory actions of omeprazole in acid environments as corrosion resistance of mild-steel. This omeprazole was characterized for its functional groups and chemical constituents using Fourier transform infra-red spectroscopy and gas chromatography. Experimental techniques and gravimetric methods were also employed. The inhibitory effects of the drug were assessed and efficiencies optimized using response surface methodology RSM, and artificial neural network ANN, models. The predominant functional groups found were C-H, C=H, C=O, C- F, and C=C stretches; C=N and N=O stretching; and N-H deformation, and contains theophylline, n-hexa-decanoic acid, di-n-octyl phthalate and methyl tetra-triacontyl ether. The Gibbs free energy results were negative, indicating the flow of heat from the inhibitor-mild-steel interface at a seemingly higher temperature to the surroundings at a lower temperature. The adsorption of the inhibitor molecules was physical and not chemisorption. The Frumkin isotherm provided the best fit and optimum efficiency of 93.71% was attained. The ANN yielded better optimization results because it had a higher value of R^2 and lower values of root-mean-square-error RMSE and standard error of prediction SEP. The impedance method displayed a capacitive loop, signifying charge-transfer process-controlled, and polarization measurements showed that the drug was a mixed-type inhibitor. Available studies have not investigated inhibitory actions of Omeprazole in acidic environments. Hence, this study aims to fill this gap and has proved Omeprazole as an excellent inhibitor for controlling mild-steel corrosion in sulphuric acid media.

Keywords: Investigate, inhibitory-action, expired omeprazole, acidic-environment.

1. Introduction

Steel is a versatile engineering material that is widely used in various applications owing to its excellent ductility, toughness, high machinability, and weldability **[22**, and **26]**. A large portion of the steel produced is utilized in chemical industrial sectors to handle salt, acid, and alkali solutions **[30]**. Although mild-steel has added to the challenge of dealing with corrosion, its continued use and popularity as an engineering material is not only based on its good mechanical properties but also on good economic advantages owing to its relative accessibility and affordability **[40]**. Thus, preserving the functionality of these metallic structures and increasing their service life depend heavily on the corrosion protection of the metallic substrates. Acid solutions used in industries cause severe corrosion of metallic structures.

Inhibitors are substances added to corrosive environments to alter the reaction between the environment and metal surface, thereby preventing or reducing corrosion. Corrosion inhibitors control or prevent corrosion via various mechanisms **[23, and 25]**.

Corrosion is simply the degradation of a substance caused by an inevitable reaction with the environment. Corrosion may also refer to the degradation of materials due to the chemical activity of their surroundings. A metal that interacts with its surroundings and sustains damage due to accidental chemical or electrochemical attacks is said to have undergone corrosion. According to **[25]**, it causes metal loss through the breakdown and loss of properties, which puts equipment safety at risk.

Since corrosion requires the maintenance and replacement of metallic structures that break prematurely, it is a significant economic loss. According to **[25]**, global corrosion damage was over 2.5 trillion dollars, or 3-4% of global GDP. More focus is placed on prevention and control as a more workable and realistic approach to minimizing the impact of corrosion damage because there are numerous factors that contribute to corrosion. These include the nature of

Vol. 10, No. 01; 2025

ISSN: 2456-3676

metals, their variability in the environment, and their applications. This ensures that corrosion is inevitable, making it difficult to eliminate **[23]**. The use of inhibitors is the most practical and dependable method to prevent corrosion under acidic and aqueous conditions **[48**, and **16]**. There has been a significant rise in the use of pharmaceutical drugs as corrosion inhibitors **[33]**. Because most drugs are synthetic forms of organic chemicals, they are environmentally benign. In acidic solutions, several medications, including irbesartan, cephapirin, ampicillin, chloramphenicol, tramadol, and sodium diclofenac salt, have been utilized as corrosion inhibitors. Consequently, expired medications should be used to profit from drug waste. The approach addresses both economic and environmental issues **[4]**. Therefore, the wide application of hydrochloric acid, potassium hydroxide etc., and metals such as carbon steel and aluminum have given the need for the present study to 'investigate the actions of expired omeprazole in sulphuric-acid as corrosion resistance of mild-steel'. However, the inability of the mild steel to form a passive layer renders it vulnerable to corrosive attacks.

According to the iron-carbon phase diagram, all binary alloys with less than 2.11 weight percent carbon are categorized as steels, and alloys with more carbon are referred to as cast iron **[47].** Iron is abundant in the Earth's crust and has the following features: high fusion temperature (1534°C), a variety of mechanical properties such as moderate yield strength (200–300 MPa) with excellent ductility to exceed the yield stress, tensile strength that can exceed 1400 MPa, and fracture toughness up to 100 MPa/M1/2.

Various criteria are used to categorize steels, including the form of component (plate, bar, strip, sheet, etc.), the deoxidation process for killed, semi-killed, and rimmed steel, and the microstructure of ferritic, austenitic, and matensitic steels. Additional factors include the heat treatment, manufacturing process, strength requirements, and finishing form **[45]**. Because chemical composition of steel has the greatest impact on all other criteria and influences how other variables affect its influence, it is the most widely used method for categorizing steel. Steel can be divided into two main groups based on its chemical makeup: alloy and carbon steel **[47]**. Steels with alloying elements purposefully added to obtain the desired qualities are known as alloy steels. Different strengthening methods, work together to give alloy steels their overall strengths **[9]**. Alloy steels are divided into two categories: low alloy-steels and stainless steel. Low-alloy steels have much better mechanical attributes such as strength and hardenability, but they are not as useful in extreme environments such as high temperatures and caustics. Stainless steel is advised under these extreme circumstances. According to **[37]**, stainless steel is an alloy steel that contains more than ten weight percent chromium and other alloying elements. These alloy steels are resistant to corrosion under a variety of chemical conditions because they contain more than 10% chromium, which forms passive oxide coating on alloy surfaces.

Matensitic, ferritic, and austenitic stainless steels are the three main varieties of stainless steels. The primary subtype of stainless steels, known as austenitic stainless steels, frequently has high concentrations of Nikel. Currently, applications requiring high corrosion resistance and exceptional mechanical qualities are dominated by austenitic stainless steels **[9]**.

Plain carbon steel; is an alloy with 2% carbon by weight. Although residual components such as silicon, manganese, and aluminum can be detected in trace amounts, no alloying element has been purposefully introduced to change or improve the properties **[11]**. When strength and other property requirements are not critical, and when high temperatures and corrosive conditions do not play a significant role in the material selection process, plain carbon steel is suitable **[24]**. Because of this, it constitutes the majority of steel used in engineering and other applications. The greatest impact on mechanical qualities is shown by variations in carbon content, where, a higher carbon content results in a higher hardness and strength. Therefore, carbon steels are typically grouped based on the amount of carbon they contain.

Because of its many uses, low-carbon steel, sometimes referred to as mild-steel, has a carbon content of 0.0005 to 0.25 weight percent. It is also known as a general-purpose steel **[25]**. Among several types of steel, those produced in the greatest quantities fall into the low-carbon category. Cold work can be used since they cannot be strengthened by heat treatment through the creation of matensite. Despite its relative softness, some of its desired qualities, such as toughness, malleability, and extraordinary ductility, are mostly due to the prevalence of ferrite and pearlite in its microstructure **[13 & 44].** Mild-steel is the preferred material for most applications owing to its excellent machinability, weldability, and comparatively low manufacturing cost. Common uses include auto body parts, which can make up 50% to 60% of weight of vehicles. Additional applications include: off-highway vehicles, ships, structures, bridges, and pressure vessels. Pipeline designers almost exclusively choose structural steels for their demanding applications, which include pipelines, gas platforms, and offshore oil installations. This is valid for pipeline systems that are used to carry materials over lengths of hundreds of feet or kilometers, such as those used to collect water, natural gas, or crude oil.

Considering the vulnerability of mild steel to corrosion, which inevitably causes significant economic losses, its availability and relatively low cost have ensured that it will continue to be in demand in engineering and industrial applications.

Over time, it has been demonstrated that the most effective method to prevent corrosion of mild steel and aluminum is the use of corrosion inhibitors. However, the use of organic and inorganic chemical corrosion inhibitors is restricted owing to high cost of their synthesis, reduced biodegradability, toxicity, and environmental hazards. Therefore, it is necessary to identify appropriate substitutes for pharmaceutical drugs that have expired. Utilizing expired medications could solve two additional delicate issues: lowering drug-related environmental pollution and reducing drug disposal expenses. The majority of expired medications contain amines, and some also have functional groups in their molecular structures such as sulfide, sulfoxide, or sulfonamide. Omeprazole was utilized in this study to regulate mild-steel corrosion in sulphuric acidic H_2SO_4 solution under various operating conditions.

Available studies have not investigated the actions of expired omeprazole drugs in acidic environments. Previous studies have explored various drugs such as pyrazinamide, isoniazid, rifampicin, atenolol, sulfamethoxazole and norfloxacin for use as mild-steel corrosion inhibitors, but the efficacy of expired omeprazole drug remains unexplored. This study aims to fill this gap by conducting experiments to evaluate the corrosion inhibition capabilities of this substance. This study aimed to provide new insights into corrosion science and pharmaceutical applications through systematic experiments and analyses.

2. Material And Methods

2.1 Materials

2.1.1 Equipment

Mild-steel used was composed of S (0.12%), Cr (0.02%), C (0.24%), Mn (0.13%), Ni (0.07), P (0.22%), Si (0.05%), and Fe (99.15%). Sulphuric-acid, H_2SO_4 was used as the acid solution in this study. Other materials include: expired omeprazole, distilled water, filter paper, thread, masking tape, emery papers, volumetric flasks, beakers, conical flasks, measuring cylinder, funnel stop-watch, thermometer, retort stand, electronic weighing balance water bath, petri-dish, oven, knife, and grinding machine. The major equipment used for instrumental analyses was the impedance electrochemical system EIS, and scanning electron microscopy SEM (-RhenomProx).

2.1.2 Preparation of H_2SO_4 Solution

1 M H_2SO_4 solution was prepared analytically using distilled water. Analytical grade acid was used. Distilled water (700ml) and 54.35 ml of H_2SO_4 were mixed in one-liter measuring cylinder and more distilled water was added to make up the solution to one liter.

2.1.3 Preparation of Concentrated Omeprazole

Different concentrations of expired drug were prepared. In each liter flask, 10g of the drug was added to make a solution of sulphuric-acid, H_2SO_4. Solutions of inhibitor were prepared at concentrations of 0.2g/L - 1.0 g/L from the stock solution.

2.1.4 Mild Steel Preparation

The 3 x 3 cm mild-steel specimens were cut into coupons. To obtain a shiny, polished surface, coupons were degreased with acetone, cleaned with distilled water, dried naturally, and placed in desiccators to eliminate any remaining oil and organic contaminants. The initial weight of each coupon was recorded with accuracy and labeled for easy identification during the corrosion control study.

2.2 Methods

2.2.1 Characterization of expired drug, omeprazole

Chemical analysis of the drug was performed. The combined features of mass spectrometry (MS) and gas chromatography (GC) were applied to identify various substances within the drug sample. When heated, the drug breaks down into separate substances. The heated materials were passed through a nitrogen-filled column to identify compounds.

2.2.2 Functional groups of the drug

High spectral resolution data over a broad range were simultaneously collected using spectrophotometer. The raw data were transformed into an actual spectrum using Fourier transform infrared FTIR. Analyses of the different FTIR-produced peaks were conducted to identify the proper functional groups **[39, and 2].** Metals were submerged in the medium while the inhibitor was present to obtain the corrosion products. In conclusion, corrosion products were gathered in beakers.

2.2.3 Weight Loss Method

2.2.3.1 Weight loss based on OFAT

The OFAT based method was applied, (varying each of the factors: temperature, time, and inhibitor concentrations, while the remaining two factors were kept constant). Using this method, 200 ml of 1 M H_2SO_4 (blank) was placed in separate 250 ml open beaker containing weighed metal coupons. Additionally, different inhibitor concentrations were added to a 250ml open beaker containing 200ml of 1 M H_2SO_4. This process was performed for each metal coupon.

From time to time, variations in weight loss were observed at different concentrations of acid solution, at different temperatures between 303K and 343K; with and without different inhibitor concentrations of 0.2g/L to 1.0g/L. The coupons were removed, submerged in acetone, cleaned, and weighed again at regular intervals.

Experimental readings were recorded. Weight loss (Δw), corrosion rate (CR), inhibition efficiency (IE) and degree of surface coverage Θ were determined with equations (2.1, 2.2, 2.3 and 2.4) respectively **[2, 50, 1, and 15]:**

$$\Delta w = w_i - w_f \qquad (2.1)$$

$$CR = \frac{w_i - w_f}{At} \qquad (2.2)$$

$$IE\% = \frac{\omega_0 - \omega_1}{\omega_0} * 100 \qquad (2.3)$$

$$\theta = \frac{\omega_0 - \omega_1}{\omega_0} \qquad (2.4)$$

Weight loss values in the presence and absence of the inhibitor are symbolized by w_1 and w_0, respectively, while w_i and w_f signify the initial and final weights of mild-steel. 'A', symbolizes mild-steel total area, 't', immersion time and Θ, surface coverage.

2.2.4 Thermodynamic properties

a) Heat of adsorption was calculated with Equation (2.5).

$$Q_{ads} = 2.303R\left[\log\left(\frac{\theta_2}{1-\theta_2}\right) - \log\left(\frac{\theta_1}{1-\theta_1}\right)\right] * \frac{T_2.T_1}{T_2-T_1} \quad (2.5)$$

where R is the gas constant, and θ_1 and θ_2 were degrees of surface coverage at temperatures T_1 and T_2, respectively.
b) Fitting experimental data to adsorption isotherms
The degree of surface coverage data was utilized for the application of various adsorption isotherms, including Flory-Huggins, Langmuir, Frumkin, and Temkin.
1. The Langmuir isotherm is expressed in Equation (2.6) **[20, 49, 50, and 15].**

$$\frac{C}{\theta} = \frac{1}{K} + C \quad (2.6)$$

C was concentration; K equilibrium constant and θ coverage; or in log form,

$$Log\left(\frac{C}{\theta}\right) = log(c) - log(k) \quad (2.7).$$

2. The Frumkin isotherm is given by Equation (2.8) **[30].**

$$\log\left((C) * \left(\frac{\theta}{1-\theta}\right)\right) = 2.303logK + 2\alpha\theta \quad (2.8)$$

where α was lateral interaction term.
3. The Temkin isotherm is expressed by Equation (2.9) **[20].**

$$\theta = -2.303logk/2\mathbf{a} - 0.303logc/2\mathbf{a} \quad (2.9)$$

where **a, was** attractive parameter.

4. The Flory-Huggins' isotherm is expressed by Equation (2.10) **[7].**

$$\log\left(\frac{\theta}{C}\right) = \log K + xlog(1-\theta) \quad (2.10)$$

where **x** was size parameter.
The Gibbs free energy of adsorption (ΔG_{ads}) was calculated using Equation (2.11) **[2].**

$$\Delta G_{ads} = -2.303RTlog(55.5K) \quad (2.11)$$

where R is the gas constant, and T is the temperature. The K values obtained from the isotherms (Langmuir, Frumkin, Temkin and Flory-Huggins' isotherms) were used to obtain the values of ΔG_{ads}.

2.2.5 Weight loss method using response surface methodology, RSM

This was used in the experimental design of the weight-loss strategy. Temperature, time, and inhibitor concentration were the variables considered; The study's response was the efficiency of the expired drug. Tables 1, and 2 display the factors and the experimental design matrix. In accordance with earlier reports **[19, and 36],** response of each case was analyzed using RSM, to further reveal the fitness of the model. Predictions regarding the responses for specific levels of each factor were made using models in terms of coded factors. High levels were coded +1 and low levels -1.

Table 1. Factors

Factor	Name	Units	Type	Minimum	Maximum	Coded Low	Coded High	Mean	Std. Dev.
A	Inhibitor concentration	g/mL	Numeric	0.6000	1.0000	-1 ↔ 0.60	+1 ↔ 1.00	0.8000	0.1451
B	Temperature	K	Numeric	303.00	323.00	-1 ↔ 303.00	+1 ↔ 323.00	313.00	7.25
C	Time	hr	Numeric	1.0000	5.00	-1 ↔ 1.00	+1 ↔ 5.00	3.00	1.45

Table 2. Experimental Design Matrix

Std	Runs	Factor A g/L	Factor B K	Factor C hr	Response (efficiency) %
4	1	1	323	1	
3	2	0.6	323	1	
13	3	0.8	313	1	
15	4	0.8	313	3	
20	5	0.8	313	3	
12	6	0.8	323	3	
1	7	0.6	303	1	
8	8	1	323	5	
5	9	0.6	303	5	
16	10	0.8	313	3	
18	11	0.8	313	3	
9	12	0.6	313	3	
14	13	0.8	313	5	
6	14	1	303	5	
19	15	0.8	313	3	
2	16	1	303	1	
17	17	0.8	313	3	
11	18	0.8	303	3	
10	19	1	313	3	
7	20	0.6	323	5	

2.2.6 Prediction of inhibition efficiency using artificial neural network (ANN)

An input-output data problem was fitted using an ANN. It involved the selection of data with neural network fitting tool, which is followed by the creation of a network **[29, and 27].** As part of the process, the network was trained and its performance evaluated. The data were categorized into three: training, validation, and testing. The network was adjusted and validated to halt training when generalization stopped improving **[29].** It stopped when there was an increase in mean square error of the validation samples. The mean-square-error (MSE) was measured as the average squared difference between the predicted outputs and actual targets. Lower values of MSE were better, as a zero value indicates no error. The statistical criterion was regression R-values, which measured the correlation between the outputs and targets.

ANN optimization involving regression analyses, performance evaluations, and training analyses, was carried out using statistical tools, as shown in Equations (2.12), (2.13), and (2.14), respectively **[27, and 31].**

$$R^2 = 1 - \frac{\sum_{i=1}^{n}(Y_{exp,i} - Y_{pred,,i})^2}{\sum_{i=1}^{n}(Y_{exp,i} - Y_{pred,,ave})^2} \quad (2.12)$$

$$RMSE = \left(\frac{1}{n}\sum_{i=1}^{n}\left(Y_{pred} - Y_{exp}\right)^2\right)^{\frac{1}{2}} \quad (2.13)$$

$$SEP = \frac{RMSE}{Y_{exp,ave}} * 100 \quad (2.14)$$

where n was number of sample points, Y_{pred}, predicted efficiency, Y_{exp}, determined efficiency, and $Y_{exp.\ ave}$, experimental average.

2.2.7 Mild-steel surface study using scanning electron microscopy (SEM)

Mild-steel samples were studied using the SEM.

2.2.8 Electrochemical Techniques

The effectiveness and type of expired drugs were determined using electrochemical techniques. Three electrodes were used in the study. The reference, counter, and working electrodes were mild-steel specimens fixed in epoxy resin and exposed to the test solution. Electrochemical measurements were performed in accordance with the methods used in **[24, and 5].**

3.0 Results and Discussion

3.1 Characteristics of expired drug: omeprazole

3.1.1 Functional groups.

The FTIR spectra of the drug are shown in Figure 1. Each spectrum shows the relationship between the transmittance and wave number representing the functional groups.

Vol. 10, No. 01; 2025

ISSN: 2456-3676

The identified functional groups are also presented in Table 3 and include: C-H and C-H bends O-H, C=C, and C-F stretches, C=N, C=O, N=O stretching and N-H deformation. The drug contained phenol, 2,4-di-tert-butylphenol, 1-Heptadecene, tridecane, and Propyl 11-octadecenoate, (heteroatoms of nitrogen and oxygen).

This table lists the peaks observed in the spectroscopic analysis of omeprazole, their intensities, and the corresponding functional groups and classes compounds.

The above details help to analyze the chemical structure and functional groups present in the compounds.

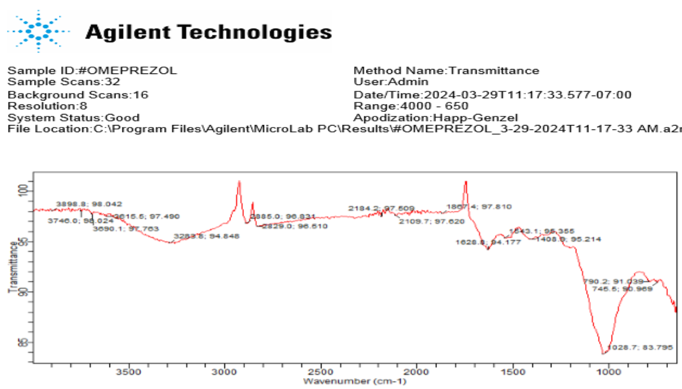

Figure 1. Spectrum of the omeprazole

Table 3. Functional groups of the omeprazole

S/N	Peaks	Intensity	Functional Group	Class of Compounds
1.	3898.8	98.042	----------------	----------------
2.	3746.0	98.024	----------------	----------------
3.	3690.1	97.763	----------------	----------------
4.	3615.5	97.490	----------------	----------------
5.	3283.8	94.848	O-H Stretch	Carboxylic Acids
6.	2885.0	96.834	C-H	Alkanes & Alkyls
7.	2829.0	96.510	C-H	Alkanes & Alkyls
8.	2184.2	97.509	C=N Stretching	Unsaturated Nitrogen compound
9.	2109.7	97.620	C=C Stretch	Alkynes
10.	1867.4	97.810	C=O Stretching	Acids Anydrides
11.	1628.8	94.177	N-H deformation	Carbonyl group
12.	1543.1	95.355	N-H deformation	Carbonyl group
13.	1408.9	95.214	N=O Stretching	Notroso compound
14.	790.2	91.039	C-H Bend	Aromatic compound
15.	745.5	90.969	C-H Bend	Aromatic compound
16.	1028.7	83.795	C-F Stretch	Alkyl Halides

3.1.2 Chemical constituents of the drug

The chemical constituents of the drugs are listed in Table 4. Omeprazole contains Undecane de-cane, dodecane, 1-(2,3-dimethylphenyl), Anethole, dodecanoic acid, tetra-decanoic acid, Carbonic acid, 1,2-benzenedicarboxylic acid, Theophylline, n-hexa-decanoic acid, 1-Octadecene, di-n-octyl phthalate, and methyl tetra-triacontyl ether. The presence of these substances shows that omeprazole has the capacity to antagonize a variety of receptors, allowing it to be used for a number of indications including corrosion inhibition, as expressed by **[22].**

Table 4. Chemical constituents of omeprazole

Peaks	Chemical Constituents
1-4	Undecane de-cane, dodecane, 1-(2,3-dimethylphenyl).
5-8	Anethole, dodecanoic acid, tetra-decanoic acid,
9-12	Carbonic acid, 1,2-benzenedicarboxylic acid.
13-16	Theophylline, n-hexa-decanoic acid
17-20	1-Octadecene, di-n-octyl phthalate, methyl tetra-triacontyl ether

3.2 Effects of Independent Factors

The effects of the process inhibitor of mild-steel in H_2SO_4 solution are presented in Table 5. The weight loss and corrosion rate decreased with increasing inhibitor concentration. The efficiency also increased with concentration. peak inhibition efficiency of 94.47% (omeprazole) was reached at 0.8g/L inhibitor concentration in 3hrs and 313K because of increase in electrostatic attraction between molecules. Beyond the maximum point, the inhibition efficiency showed slight decrease. The observed retardation may be due to the force of attraction between the molecules of the inhibitor and surface of mild-steel **[38, 1, 46, and 43].** weight loss and corrosion rate increased with temperature. Consequently, an increase in temperature decreases the efficiency levels of omeprazole as an inhibitor may be due to the force of mild-steel **[52, 46, and 10].**

The inhibition efficiency increased with time. It collaborates with the reports of previous research works **[24, 6, and 49],** which stated that the efficiency of the inhibitor improves with time. The high inhibition efficiency may be due to viable hetero-atom.

3.3 Effects of the Independent Factors

Table 5. *Effects of the Independent Factors* Effect of **Time**

Time (hr)	ΔW_0 (g)	CR_0 (mg/cm^2hr)	ΔW_1 (g)	CR_1 (mg/cm^2hr)	IE (%)	ϴ
1	0.157	17.44	0.024	2.667	84.71	0.8471
2	0.308	17.11	0.027	1.500	91.23	0.9123
3	0.506	18.74	0.028	1.037	94.47	0.9447
4	0.511	14.19	0.035	0.972	93.15	0.9315
5	0.527	11.71	0.038	0.844	92.79	0.9279
Effect of **concentration**						
0.0	0.506	18.74				
0.2			0.161	5.963	68.18	0.6818
0.4			0.126	4.667	75.10	0.7510
0.6			0.097	3.593	80.83	0.8083
0.8			0.028	1.037	94.47	0.9447
1.0			0.041	1.519	91.90	0.9190
Effect of **temperature**						
303	0.422	15.63	0.037	1.370	91.23	0.9123
313	0.506	18.74	0.028	1.037	94.47	0.9447
323	0.557	20.63	0.077	2.852	86.18	0.8618
333	0.722	26.74	0.140	5.185	80.61	0.8061
343	0.810	30.00	0.192	7.111	76.30	0.7630

3.3.1 Heat of adsorption

The heat of adsorption (Q_{ads}) for corrosion control is presented in Table 6. Q_{ads} had negative values for all concentrations ranging from 0.2g/L to 1.0g/L. This means that adsorption was accompanied by the release of heat. This was similar to the reports of **[52,** and **22]**, where a negative value for the heat of adsorption was an indication of an exothermic process. The status of Q_{ads} showed flow of heat from the inhibitor mild-steel interface at a seemingly higher temperature to the surroundings at a lower temperature.

Table 6. Heat of adsorption for corrosion control in H_2SO_4 using omeprazole

Concentration (g/L)	Heat of adsorption, Q_{ads} (J/mol)
	Omeprazole
0.2	-63762.5
0.4	-65085.8
0.6	-74242.6
0.8	-84722.3
1.0	-58890

3.3.2 Adsorption Results

The results of these parameters are listed in Table 7. The Frumkin isotherm was the best-fitted isotherm. This assertion was based on the recorded highest average value of the coefficient of determination (R^2); which was closest to the critical value of 1 (one) compared to the R^2 values of the other isotherms (Langmuir, Temkin and Flory-Huggins). In the Temkin results, the attractive parameter (a) values were negative implying no chemical reaction between mild steel and omeprazole. The lateral interaction term (α) at 313K and 323K was positive. This means there was a noticeable attraction between omeprazole and mild-the steel surface. Positive values of size property (x), were revealed by analysis of the Flory-Huggins' isotherm, indicating reasonable layer of drug attachment to the mild-steel. Gibb's free energy was lower than -40.00kJ/mol, hence adsorption was physical **[2,** and **41].**

Table 7. Results of *Adsorption* parameters

Isotherms	Temperatures (K)	R^2	K	ΔG_{ads} (J/mol)	Properties	
Langmuir	313	0.9939	0.9192	-10218.7		
	323	0.964	0.8441	-1`0219.3		
Temkin	313	0.8938	274.73	-10312.2	a	-3.0262
	323	0.847	35.5959	-10545.2		-2.1293
Frumkin	313	0.9977	0.0130	-10234.3	α	2.8813
	323	0.9814	0.0818	-10286.1		1.9004
Flory-Huggins	313	0.6762	4.5300	-10234.3	x	0.5542
	323	0.5786	2.5474	-10332.5		0.5297

3.3.3 Optimization Results

The RSM results and optimization data are listed in Table 8, maximum value of efficiency was 94.46% at 0.8g/L, 313K and 3hrs. This indicates that effects of the variables are parabolic and conform with the quadratic model **[2,** and **41].**

Table 8. RSM results

Std	Runs	Factor A g/L	Factor B K	Factor C hr	Response (efficiency) %
4	1	1	323	1	62.54
3	2	0.6	323	1	47.83
13	3	0.8	313	1	85.81
15	4	0.8	313	3	94.46
20	5	0.8	313	3	94.46
12	6	0.8	323	3	79.36
1	7	0.6	303	1	61.62
8	8	1	323	5	77.47
5	9	0.6	303	5	64.56
16	10	0.8	313	3	94.46
18	11	0.8	313	3	94.46
9	12	0.6	313	3	79.28
14	13	0.8	313	5	92.09
6	14	1	303	5	79.52
19	15	0.8	313	3	94.46
2	16	1	303	1	70.67
17	17	0.8	313	3	94.46
11	18	0.8	303	3	88.15
10	19	1	313	3	88.69
7	20	0.6	323	5	54.44

3.3.4 Quadratic models' ANOVA

The ANOVAs of the quadratic models' ANOVA were shown in Table 9 for the omeprazole efficiency in H_2SO_4 solution.

Table 9. Quadratic models' ANOVA for the omeprazole efficiency in H_2SO_4 solution

Source	Sum of Sqs	df	Mean Sq	F-value	p-value	
Model	4219.50	9	468.83	226.05	< 0.0001	Sig
A	506.37	1	506.37	244.15	< 0.0001	
B	183.87	1	183.87	88.65	< 0.0001	
C	156.90	1	156.90	75.65	< 0.0001	
AB	23.56	1	23.56	11.36	0.0071	
AC	25.31	1	25.31	12.20	0.0058	
BC	11.88	1	11.88	5.73	0.0377	
A^2	366.45	1	366.45	176.68	< 0.0001	
B^2	381.20	1	381.20	183.79	< 0.0001	
C^2	119.02	1	119.02	57.38	< 0.0001	
Residual	20.74	10	2.07			
Lack of Fit	20.74	5	4.15			
Pure Error	0.0000	5	0.0000			
Cor Total	4240.24	19				
Std. Dev.	1.44		R^2		0.9951	
Mean	79.94		Adj R^2		0.9907	
C.V. %	1.80		Pred R^2		0.9625	
			Adeq Pre		45.5809	

3.3.5 Quadratic model of inhibition efficiency of omeprazole

The generated models were quadratic. The coded equation was useful in identifying the relative impact of the factors by comparing the coefficients. The equation in terms of actual factors can be used to predict responses for each factor, but the levels should be specified in the original units. The equation in terms of actual factors should not be used to determine the relative impact of each factor because the coefficients were scaled to accommodate the units of each factor and the intercept was not at the center of the design space.

3.3.6 Diagnostic report

Equation of coded factors for omeprazole in H_2SO_4

$$\text{Inhibitor efficiency} = + 94.89 + 7.12A - 4.29B + 3.96C + 1.72AB + 1.78AC + 1.22BC - 11.54A^2 - 11.77B^2 - 6.58C^2 \quad (3.1)$$

Equation of actual factors for omeprazole in H_2SO_4

$$\text{Inhibitor efficiency} = -11256.55026 + 215.39170 \text{ inhibitor concentration} + 72.40485 \text{ temperature} - 10.78248 \text{ time} + 0.858125 \text{ inhibitor concentration} \times \text{temperature} + 4.44687 \text{ inhibitor concentration} \times \text{time} + 0.060937 \text{ temperature} \times \text{time} - 288.59091 \text{ inhibitor concentration}^2 - 0.117736 \text{temperature}^2 - 1.64466 \text{time}^2 \quad (3.2)$$

Table 10 presents report of the diagnostic analysis for corrosion control using omeprazole. Predicted, residual, leverage, difference in fit (DFFIT) and Cook's distance were determined. A graphical analysis of the predicted versus actual inhibition efficiencies of the drug were presented in Figure 2. These are linear graphs, where points are huddled along the line of the best fit. This figure also shows the generated data.

Table 10. Report for the omeprazole efficiency in H_2SO_4

Run Order	Actual Value	Predicted Value	Residual	Leverage	Internally Studentized Residuals	Externally Studentized Residuals	Cook's Distance	Influence on Fitted Value DFFITS	Standard Order
1	62.54	62.58	-0.0373	0.793	-0.057	-0.054	0.001	-0.106	4
2	47.83	48.47	-0.6403	0.793	-0.978	-0.975	0.367	-1.910	3
3	85.81	84.35	1.46	0.491	1.423	1.512	0.195	1.484	13
4	94.46	94.89	-0.4275	0.118	-0.316	-0.301	0.001	-0.110	15
5	94.46	94.89	-0.4275	0.118	-0.316	-0.301	0.001	-0.110	20
6	79.36	78.83	0.5342	0.491	0.520	0.500	0.026	0.491	12
7	61.62	62.92	-1.30	0.793	-1.979	-2.408	1.502	-4.715	1
8	77.47	76.49	0.9757	0.793	1.490	1.602	0.851	3.138	8
9	64.56	64.84	-0.2833	0.793	-0.433	-0.414	0.072	-0.811	5
10	94.46	94.89	-0.4275	0.118	-0.316	-0.301	0.001	-0.110	16
11	94.46	94.89	-0.4275	0.118	-0.316	-0.301	0.001	-0.110	18
12	79.28	76.23	3.05	0.491	2.970	8.213	0.851	8.065	9
13	92.09	92.27	-0.1798	0.491	-0.175	-0.166	0.003	-0.163	14
14	79.52	79.20	0.3197	0.793	0.488	0.469	0.091	0.918	6
15	94.46	94.89	-0.4275	0.118	-0.316	-0.301	0.001	-0.110	19
16	70.67	70.16	0.5117	0.793	0.781	0.765	0.234	1.498	2
17	94.46	94.89	-0.4275	0.118	-0.316	-0.301	0.001	-0.110	17
18	88.15	87.40	0.7482	0.491	0.728	0.710	0.051	0.697	11
19	88.69	90.46	-1.77	0.491	-1.722	-1.948	0.286	-1.913	10

20	54.44	55.27	-0.8323	0.793	-1.271	-1.317	0.619	-2.578	7

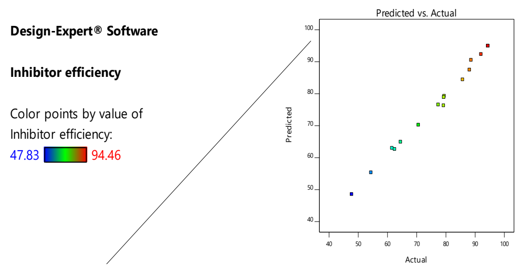

Figure 2. Predicted against actual efficiency of omeprazole in H_2SO_4

3.3.7 Three dimensional 3-D plots of omeprazole

3-D plots of RSM analysis of the efficiencies of the inhibitors are presented in Figure 3. The interactive effects of the independent factors on the dependent variable displayed parabolic curves in all cases. The nature of the graphs (parabolic curves) supports the earlier explanation that the quadratic model fits the factors. In addition, 3-D plots showcased optimum parameters as determined by the optimization tool.

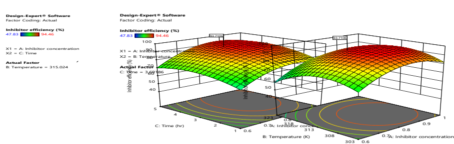

(a) (b)

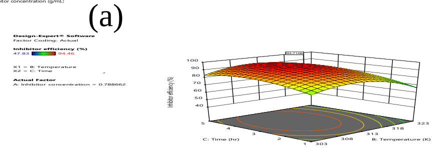

(c)

Figure 3. Efficiency versus (a) temperature and concentration of omeprazole in H_2SO_4 (b) time and concentration of omeprazole in H_2SO_4 and (c) time and temperature of omeprazole in H_2SO_4

3.3.8 Optimum results of RSM

The optimum values of the corrosion control parameters are presented in Table 11. In H_2SO_4 solution, omeprazole had higher efficiency of 93.71%. This may be due to the higher quality of the phytochemicals and the intensity of the functional groups. The recorded high efficiencies show that Omeprazole is suitable for controlling mild-steel corrosion in acid solutions.

Table 11. Optimum results of the corrosion inhibition process

Media	Opt. conc. (g/L)	Opt. temp. (k)	Opt. time (hrs)	Opt. IE (%)
Mild steel in H_2SO_4 with omeprazole	0.79	315.02	3.69	93.71

3.3.9 Validation of results

Table 12 presents the validation of the RSM results. At optimum conditions, the predicted and experimental values of the inhibition efficiency were compared using the percentage deviation as a statistical tool. Recorded values were less than 5% hence, the model effectively predicted the experimental data.

Table 12. Validation of results

Media	Opt. conc. (g/L)	Opt. temp. (k)	Opt. time (hrs)	Opt. IE (%)	Exp. IE (%)	Percentage deviation (%)
Mild steel in H_2SO_4 with omeprazole	0.79	315.02	3.69	93.71	93.45	0.28

3.3.10 ANN results

The ANN results for corrosion control are presented using the regression evaluation graphs in Figure 4. Validation and testing were performed on the graphical results. Points of the training data were clustered on the line of the best fit. Statistical analysis of the performance in terms of the mean square error and correlation of determination are equally presented.

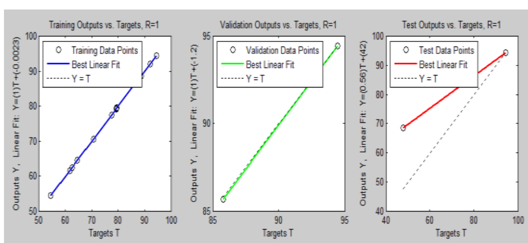

(a) (b) (c)

Figure 4. ANN regression for prediction of efficiency of omeprazole in H_2SO_4: (a) training output, (b) validation output, (c) test output.

3.3.11 RSM and ANN Results of Corrosion Control.

The RSM and ANN results of corrosion control using omeprazole are presented in Table 13. The experimental, RSM predicted and ANN predicted efficiencies are reported as functions of time, temperature and concentration.

Table 13. RSM and ANN results of omeprazole efficiency in H_2SO_4.

Std	Run	F 1 A: Inh. conc. g/L	F 2 B: Temp. K	F 3 C: Time hr	Actual IE (%)	RSM predicted IE (%)	ANN predicted IE (%)
4	1	1	323	1	62.54	62.58	62.54
3	2	0.6	323	1	47.83	48.47	47.83
13	3	0.8	313	1	85.81	84.35	85.81
15	4	0.8	313	3	94.46	94.89	94.46
20	5	0.8	313	3	94.46	94.89	94.46
12	6	0.8	323	3	79.36	78.83	79.36
1	7	0.6	303	1	61.62	62.92	61.62
8	8	1	323	5	77.47	76.49	77.47
5	9	0.6	303	5	64.56	64.84	64.56
16	10	0.8	313	3	94.46	94.89	94.46
18	11	0.8	313	3	94.46	94.89	94.46
9	12	0.6	313	3	79.28	76.23	79.28
14	13	0.8	313	5	92.09	92.27	92.09
6	14	1	303	5	79.52	79.2	79.52
19	15	0.8	313	3	94.46	94.89	94.46
2	16	1	303	1	70.67	70.16	70.67
17	17	0.8	313	3	94.46	94.89	94.46
11	18	0.8	303	3	88.15	87.4	88.15
10	19	1	313	3	88.69	90.46	88.69
7	20	0.6	323	5	54.44	55.27	54.44

F 1 Inh. conc F 2 Temp. F 3 Time

3.2.12 Comparison of ANN and RSM results.

The comparative results of the ANN and RSM in terms of RMSE, SEP, and R^2 are presented in Table 14. ANN had a smaller root-mean-square-error (RMSE) and standard error of prediction (SEP). This observation showed a better prediction than RSM, which is in line with previous studies **[29, 27,** and **24],** where the superiority of ANN over RSM was mentioned. Basis on the correlation of determination (R^2), the ANN also had a higher value. Thus, ANN performed better than RSM in predicting the efficiency of omeprazole inhibitor.

Vol. 10, No. 01; 2025

ISSN: 2456-3676

Table 14. Comparison of the predictions of ANN and RSM in terms of RMSE, SEP and R^2.

Comparison of Prediction	RMSE	SEP	R^2
RSM	1.01842	1.273989	0.986343
ANN	0.0023	0.002877	1

3.3.13 SEM-EDX results

The SEM-EDX results are presented in Figures 5a and 5b, where the surface morphologies of mild-steel, were subjected to corrosion in uninhibited and inhibited H_2SO_4 solution. The mild-steel in Figure 5a in the uninhibited solution was deeply corroded compared with the inhibited solutions in Figure 5b, which had a lesser corrosion impact. Observations are in line with the findings of **[2],** which stated that metal was more seriously damaged in an uninhibited medium than in an inhibited medium. The results show changes in the elemental compositions of mild-steel surface. The effective corrosion control of mild-steel in acid solutions using omeprazole was established by revealing of the morphological results.

The mild-steel in Figure 5a has the following elements with their numbers, symbols, atomic concentrations and weight concentrations in the order of: Fe 26, 24.06 and 55.29; Carbon C 6, 69.35 and 34.28; Silicon Si 14, 1.50 and 1.73; Chlorine Cl 17, 1.41 and 2.06; Aluminum Al 13, 2.02 and 2.25; Tin Sn 50, 0.21 and 1.02; Manganese Mn 0.10, 0.23 and 0.66; Sulfur S 16, 0.30 and 0.33; Titanium Ti 22, 0.15 and 0.25; Phosphorus P 15, 0.35 and 0.45; Vanadium V 23, 0.21 and 0.41; Nickel Ni 28, 0.00 and 0.00; and Chromium Cr 24, 0.13 and 0.29. Similarly, in Figure 5 (b) the mild-steel had the following elements: Iron Fe 26, 28.11 and 61.54; Carbon C 6, 66.92 and 31.51; Silicon Si 14, 1.73 and 1.91; Aluminum Al 13, 1.16 and 1.23; Tin Sn 50, 0.15 and 0.71; Chlorine Cl 17, 0.54 and 0.75; Sulfur S 16, 0.29 and 0.36; Phosphorus P 15, 0.29 and 0.33; Nickel Ni 28, 0.00 and 0.00; Chromium Cr 24, 0.16 and 0.33; Vanadium V 23, 0.06 and 0.12; Titanium Ti 22, 0.27 and 0.51; and Manganese Mn 25, 0.29 and 0.35.

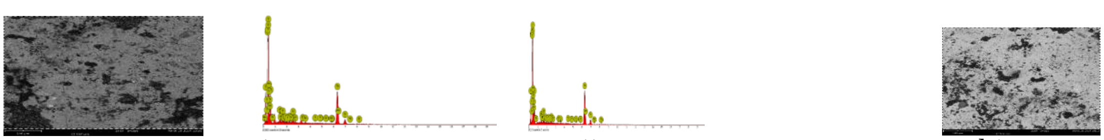

ai aii bi bii

Figure 5. SEM-EDX result of omeprazole: (a) (i and ii) in uninhibited H_2SO_4 (b) (i and ii) in inhibited H_2SO_4.

3.3.14 Electrochemical Results

The electrochemical results presented in Figures 6a and 6b, are for impedance spectroscopy and potentio-dynamic polarization, respectively. Higher inhibitor concentrations produced larger capacitive loops in inhibited solution indicating that the mild-steel had a higher corrosion resistance in presence of the inhibitor. Impedance spectroscopic technique (EIS) exhibits capacitive loop indicating a charge-transfer process-controlled corrosion reaction **[14]** and **[52].**

Increased inhibitor concentration inhibited anodic and cathodic reactions as observed from polarization curves, indicating that omeprazole was a mixed-type inhibitor.

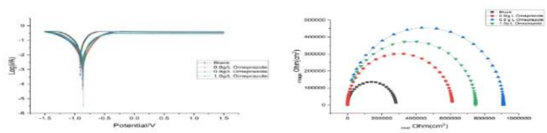

(a) PDP (b) EIS

Figure 6. Electrochemical results in blank and inhibited H_2SO_4 solution (a) PDP (b) EIS

4.0 Conclusion

- This work investigated the inhibition properties of Omeprazole as an inhibitor for mild steel corrosion in H_2SO_4 media.
- The predominant functional groups of the drug were the C-H and C-H bends O-H, C=C, and C-F stretches, C=N, C=O, N=O stretching and N-H deformation. The drug contained nitrogen and oxygen heteroatoms.
- Omeprazole in H_2SO_4 medium can be used to inhibit corrosion of mild-steel
- The status of Q_{ads} was negative, which showed that there was a flow of heat from the inhibitor-mild-steel interface of seemingly higher temperature to the surroundings of lower temperature. The adsorption of the inhibitors' molecules was physical, not chemisorption, and Frumkin isotherm was the best fit.
- quadratic model adequately described relationships between efficiency and factors of inhibitor and optimum efficiency of 93.71% was attained. ANN gave better optimization result than the RSM because ANN had higher R^2 and lower RMSE and SEP.
- From the results of electrochemical impedance spectroscopy, charge-transfer characterized the corrosion process. Omeprazole was seen as mixed-type inhibitor in corrosive media.

"Statements and Declarations"

- **Declaration of Competing Interest:**
- The authors declare that they have no known competing financial interests or personal relationships that could have influenced the work in this study.

- **Funding Statement:**
- All authors certify that they have no affiliations with or involvement in any organization or entity with any financial interest or non-financial interest in the subject matter or materials discussed in this manuscript.

Declaration of Ethical Statement:

This research received ethical approval, and complied with the guidelines and regulations of the studies. Informed consent was obtained from all participants. There were no human participants involved in the study.

- Therefore, the research has been conducted with the highest standards for rigor and integrity.

- The article study is original.
- This work has not been submitted elsewhere and is not under consideration for publication elsewhere.
- The work does not include libelous, defamatory or unlawful statements.
- There was no third-party material(s) included.
- Proof of consent has been obtained for any named individuals or organizations.
- Authorship has been agreed prior to submission and no one has been 'gifted' authorship or denied credit as an author (ghost authorship).

Data Availability: No data was used in this article. However, the data that support the findings of this study are available from the corresponding author, [J. I. O], upon reasonable request.

References

Anadebe, V.C., Onukwuli, O. D., Omotioma, M., Okafor, N. A. (2019). Experimental theoretical modeling and optimization of inhibition efficiency of pigeon pea leaf extract as anti-corrosion agent of mild steel in acid environment. *Material Chemistry and Physics*, 233: 120-132.

Anadebe, V.C., Onukwuli, O. D., Omotioma, M., Okafor, N. A. (2018). Optimization and electrochemical study on the control of mild steel corrosion in hydrochloric acid solution with bitter kola leaf extract as inhibitor. *S. Afr. J. Chem*. 71: 51-61.

Azeez, F. A., Al-Rashed, O. A., Nazeer, A. A. (2018). Controlling of mild steel corrosion in acidic solution using environmentally friendly ionic liquid inhibitors: Effect of alkyl chain. *Journal of Molecular Liquids*, 265: 654-663.

Bhadeshia, H., Honeycombe, R. (2017). Steels: Microstructure and properties. Butterworth-Heinemann.

Chigondo, M., and Chigondo, F. (2016). Recent natural corrosion inhibitors for low carbon steel: An overview. Journal of Chemistry.

Deyab, M. A. (2020). Understanding the anti-corrosion mechanism and performance of ionic liquids in desalination, petroleum, pickling, de-scaling, and acid cleaning applications. *Journal of Molecular Liquids*, *309*(1): 113107–113139.

Ezeugo, J. N. O., Onukwuli, O. D., Omotioma, M. (2017). Optimization of corrosion inhibition of *Picralima nitida* leaves extract as green corrosion inhibitor for zinc in 1.0 M HCl. *World News of Natural Sciences*, 15: 139-161.

Furniss, B. S., Hannaford, A. J., Smith, P. W. G., Tatchell, A. R. (1989). Vogel's Textbook of Practical Organic Chemistry (5th ed.). Longman.

Fouda, A. S., Ahmed, A. M., El-Darier, S. M., Ibrahim, I. M. (2021). *Wihanias* omnifera extract as a friendly corrosion inhibitor of carbon steel in HCl solution. *International Journal of Corrosion and Scale Inhibition*, *10*(1): 245–261.

Fouda, A. S., Mahmoud, W. M., Abdul Mageed, H. A. (2016). Evaluation of an expired nontoxic amlodipine besylate drug as a corrosion inhibitor for low-carbon steel in hydrochloric acid solutions, J. Bio- Tribo-Corros., 2 (2), 7.

Vol. 10, No. 01; 2025

ISSN: 2456-3676

Iannuzzi, M., and Frankel, G. S. (2022). The carbon footprint of steel corrosion. npj Materials Degradation, 6(1), 101.

Islam, T., and Rashed, H. M. (2019). Classification and application of plain carbon steels.

Kakani, S. L., and Kakani, A. (2004). Material Science. New Age International. New Delh

Karthik, G., and Sundaravadivelu, M. (2016). Studies on the inhibition of mild steel corrosion in hydrochloric acid solution by atenolol drug. *Egyptian Journal of Petroleum*, *25*(2): 183-191.

Morales, E. V. (2011). Alloy steel: Properties and use. (Ed.) BoD–Books on Demand

Nnanwube, I. A., and Onukwuli, D. O. (2020). Modeling and optimization of galena dissolution in a binary solution of nitric acid and ferric chloride using artificial neural network coupled with genetic algorithm and response surface methodology, *South African Journal of Chemical Engineering*, 32: 68-77.

Noor, E. A., Al-Moubaraki, A. H. (2008). Thermodynamic study of metal corrosion and adsorption process in mild steel/ 1-methyl-4/4 (-x) – stryrul pyridinium iodide/ hydrochric acid inhibitor system, material chemistry and physics, vol.110, no 1

Omotioma, M., and Onukwuli, O. D. (2016a). Corrosion inhibition of mild steel in 1.0M HCl with castor oil extract as inhibitor, *Int. J. Chem. Sci*., 14(1), 103-127.

Omotioma, M., and Onukwuli, O. D. (2016b). Modeling the corrosion inhibition of mild steel in HCl medium with the inhibitor of pawpaw leaves extract, *Portugaliae Electrochemical Acta*, 34 (4): 287-294.

Omotioma, M., and Onukwuli, O. D. (2017). Evaluation of pawpaw leaves extract as anti-corrosion agent for aluminium in hydrochloric acid medium, *Nigerian Journal of Technology (NIJOTECH)*, 36 (2): 496-504.

Omotioma, M., Onukwuli, O. D., Obiora-Okafo, I. (2019). Phytochemicals and inhibitive properties of cashew extract as corrosion inhibitor of aluminum in H_2SO_4 medium *Latin American Applied Research*, 49: 99-103.

Omotioma, M., Green, T. B., Okorie, O., Ekete, J. A., Aliozo, O. S. (2024a). Gravimetric study of corrosion inhibition of mild steel in H_2SO_4 environment using watermelon (*Citrullus lanatus* (Thunb.) Matsum. & Nakai) leaf extract as inhibitor. *World News of Natural Sciences*, *53*: 17-31.

Omotioma, M., Okolo, N. W., Okorie, O., Ekete, J. A., Aliozo, O. S. (2024b). Corrosion control of mild steel in hydrochloric acid solution using extract of sweet potato leaf as green inhibitor. *World Scientific News*, (189): 23-37.

[24] Omotioma, M., Onukwuli, O. D., Nnanwube, I. A. (2024c). Testing the inhibition efficiency of the castor oil leaf as corrosion inhibitor of mild steel in H_2SO_4. *Heliyon*.DOI:https: //doi.org/10.1016/j. Heliyon. e31168

Onukwuli, O. D., Omotioma, M. (2016). Optimization of the inhibition efficiency of mango extract as corrosion inhibitor of mild steel in 1.0M H_2SO_4 using response surface methodology, *Journal of Chemical Technology and Metallurgy*, 51 (3): 302-314.

Onukwuli, O. D., Udeh, B. C., Omotioma, M., Nnanwube, I. A. (2021). Corrosion inhibition of aluminum in hydrochloric acid medium using cimetidine as inhibitor: Empirical and optimization studies, *Anti-corrosion methods and materials*, 68(5): 385-395.

Onukwuli, O. D., and Omotioma, M. (2019). Study of bitter leaves extract as inhibitive agent in HCl medium for the treatment of mild steel through pickling, *Portuagaliae Electrochemical Acta*, 37 (2): 115-121.

Pathak, R. K., and Mishra, P. (2016). Drugs as corrosion inhibitors: A Review. Inter. J. Sci. Res., 5: 669–671.

Paul, P. K., Yadav, M., Obot, I. B. (2020). Investigation on corrosion protection behaviour and adsorption of carbon-hydrazide-pyrazole compounds on mild steel in 15% HCl solution: Electrochemical and computational approach. *Journal of Molecular Liquids*, 314,11313.

Pilkington, J., Preston, C., Gomes, R. L. (2014). Comparison of response surface methodology (RSM) and artificial neural network (ANN) towards efficient extraction of *artemisinin* from *Artemisia Annua*, *Industrial Crops and Products*, 58: 15-24.

Popova, A., Christov, M., Vasilev, A. (2015). Mono-and di-catonic benzothiazolic quaternary ammonium bromides as mild steel inhibitors, part III: Influence of the temperature on the inhibitor process. *Corrosion Science*, 94: 70-78.

Pramani, A., and Basak, A. K. (2015). Stainless steel: microstructure, mechanical properties and methods of application. Nova Science Publishers (Eds.), Incorporated. Proceedings, 24: 1174-1182

Qurishi, M. A., Chauhan, D. S., Saji, V. S. (2021). Heterocyclic biomolecules as green corrosion inhibitors, *Journal of Molecular Liquids*, 341, 117265.

Rani, B. E., and Basu, B. B. J. (2012). Green inhibitors for corrosion protection of metals and alloys: An overview. *International Journal of corrosion*.

Revie, R. W., and Uhlig, H. H. (2008). Corrosion and corrosion control: An introduction to corrosion science and engineering" a John Wiley & Sons. INC., publication.

Sheatty, D. S., Shetty, P., Nayak, H. V. S. (2006). Journal Chidean Chemical Society 51, 849 Singh A, Gupta A, Rawat AK, Ansari KR, Quraishi MA Ebenso EE (2014) Cimetidine as an effective corrosion inhibitor for mild steel in hydrochloric acid, *International Journal of Electrochemical Science*, 9(12): 7614-7628.

Singh, R. (2012). Classification of Steels. Appl. Weld. Eng, 51-56.

Smil, V. (2016). Still the iron age: Iron and steel in the modern world. Butterworth Heinemann.

Solomon, M. M., Umoren, S. A. (2015). Enhanced corrosion inhibition effect of polypropylene glycol in the presence of iodide ions at mild steel/sulphuric acid interface. *Journal of Environmental Chemical Engineering*, 3(3): 1812-1826

Speller, F. N. (1951). Corrosion causes and prevention, McGraw- Hill Book Co., Inc, New-York and London.

Totten, G. E. (2006). Steel heat treatment: Metallurgy and technologies. CRC (Ed.) press.

Udeh, B. C., Onukwuli, O. D., Omotioma, M. (2021). Application of metronidazole drug as corrosion inhibitor of mild steel in hydrochloric acid medium, *Journal of Engineering and Applied Sciences*, 18(1): 329-347.

Umoren, S. A., Eduok, U. M., Solomon, M. M., Udoh, A. P. (2016). Corrosion inhibition by leaves and stem extracts of *Sida acuta* for mild steel in 1M H_2SO_4 solutions investigated by chemical and spectroscopic techniques. *Arab. J Chem.*, 9, 209-224.

Vengatesh, G., Karthik, G., Sundaravadivelu, M. (2017). A comprehensive study of ondansetron hydrochloride drug as a green corrosion inhibitor for mild steel in 1 M HCl medium. *Egyptian Journal of Petroleum*, *26*(3): 705-719.

Verma, C., Quarishi, M. A., Ebenso, E. E., Obot, I. B., El-Assyry, A. (2016). 3-Amino alkylated indoles as corrosion inhibitors for mild steel in 1M HCL: Experimental and theoretical studies. *Journal of Molecular Liquids*, 219: 647-660

Smil, V. (2016). Still the iron age: Iron and steel in the modern world. Butterworth Heinemann.

Solomon & Umoren, (2015). Enhanced corrosion inhibition effect of polypropylene glycol in the presence of iodide ions at mild steel/sulphuric acid interface. *Journal of Environmental Chemical Engineering*, 3(3), pp.1812-1826

Udeh, B. C., Onukwuli, O. D., Omotioma, M. (2021). Application of metronidazole drug as corrosion inhibitor of mild steel in hydrochloric acid medium, *Journal of Engineering and Applied Sciences*, 18(1): 329-347.

Umoren, S. A., Eduok, U. M., Solomon, M. M., Udoh, A. P. (2016). Corrosion inhibition by leaves and stem extracts of *Sida acuta* for mild steel in 1M H_2SO_4 solutions investigated by chemical and spectroscopic techniques. *Arab. J Chem*., 9, 209-224.

Vengatesh, G., Karthik, G., Sundaravadivelu, M. (2017). A comprehensive study of ondansetron hydrochloride drug as a green corrosion inhibitor for mild steel in 1 M HCl medium. *Egyptian Journal of Petroleum*, *26*(3): 705-719.

Verma, C., Quarishi, M. A., Ebenso, E. E., Obot, I. B., El-Assyry, A. (2016). 3-Amino alkylated indoles as corrosion inhibitors for mild steel in 1M HCL: Experimental and theoretical studies. *Journal of Molecular Liquids*, 219: 647-660.